

Supporting Information

Spectroscopy and dynamics of a HOF and its molecular units: remarkable vapors acid sensing

Eduardo Gomez^a, Yuto Suzuki^b, Ichiro Hisaki^c, Miquel Moreno^d, Abderrazzak Douhal^{a}*

^aDepartamento de Química Física, Facultad de Ciencias Ambientales y Bioquímica, and INAMOL, Universidad de Castilla-La Mancha, Avenida Carlos III, S.N., 45071 Toledo, Spain.

^bGraduate School of Engineering, Osaka University, 2-1 Yamadaoka, Suita, Osaka 565-0871, Japan

^cResearch Institute for Electronic Science, Hokkaido University, Kitaku, Sapporo, Hokkaido 001-0020, Japan.

^dDepartament de Química, Universitat Autònoma de Barcelona, Bellaterra, 08193 Barcelona, Spain.

*Corresponding author: E-mail address: abderrazzak.douhal@uclm.es

Molecule	State	Energy ^a	Charge of the core ^b	μ ^c	λ ^d
CPHAT	S ₀	0.0 (0.0)	0.71 (-0.36)	8.07 (4.64)	- (-)
	S _{1,FC}	88.5 (89.8)	0.66 (-0.40)	7.79 (4.65)	323 (320)
	S ₁	75.0 (83.0)	0.88 (-0.43)	5.62 (4.04)	438 (392)
	T ₁	59.2 (59.1)	0.70 (-0.30)	4.84 (2.09)	483 (1808)
CBPHAT	S ₀	0.0 (0.0)	0.66 (-0.39)	1.66 (1.11)	- (-)
	S _{1,FC}	85.4 (87.7)	0.60 (-0.56)	2.60 (1.15)	335 (326)
	S ₁	75.3 (79.2)	0.92 (-0.50)	5.09 (2.90)	454 (412)
	T ₁	58.0 (57.8)	0.90 (-0.38)	4.74 (2.61)	493 (1803)

Table S1. Theoretical values of the energies, electronic charges on the core, dipole moments and wavelengths of absorption from S₀ to the indicated electronic states, in gas phase and using the continuum model (DMF as solvent). The numbers between parenthesis correspond to the ones obtained in gas phase. ^a Relative energy in kcal/mol. ^b Electronic Charge in a.u. ^c Dipole moment in Debye. ^d Wavelength in nm.

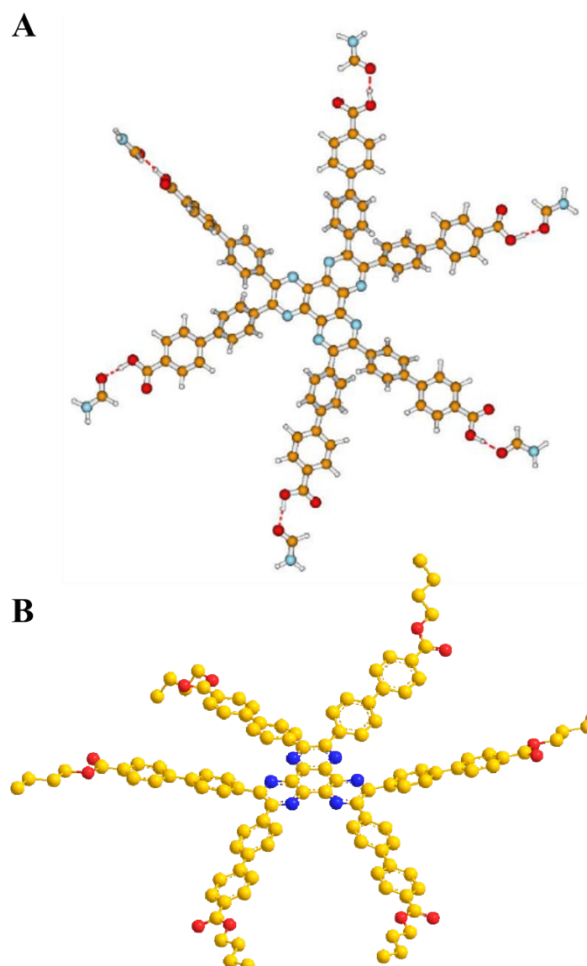


Figure S1. A) Optimized molecular structure of CBPHAT interacting with 6 molecules of DMF. B) The most stable conformation of CBPHAT-C₄H₉.

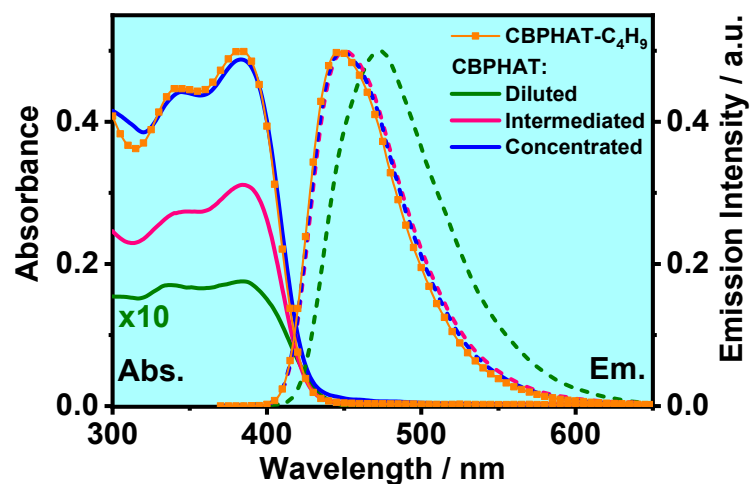


Figure S2. UV-visible absorption and emission spectra of CBPHAT- C_4H_9 and CBPHAT at different concentrations in DMF solutions. The excitation wavelength was emission spectra is 350 nm. For diluted, intermediate and concentrated samples of CBPHAT in DMF solutions, the OD at 383 nm are 0.017, 0.31 and 0.48, respectively.

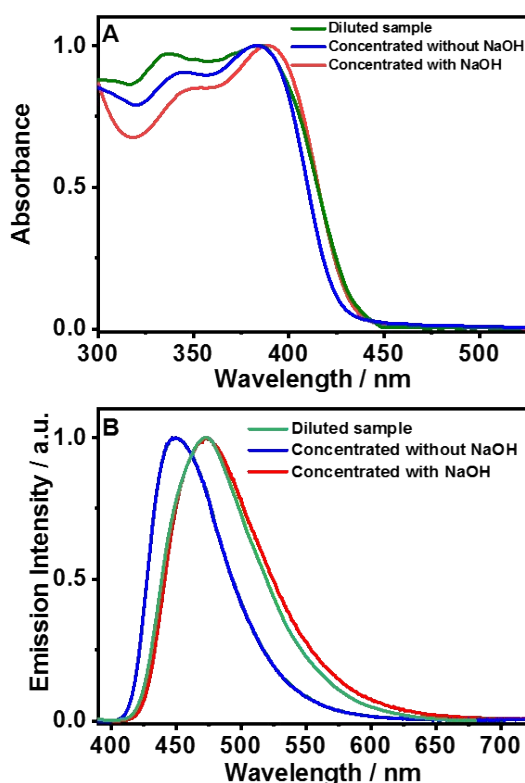


Figure S3. Normalized to the maximum intensity A) UV-visible absorption and B) emission spectra of diluted (OD (383 nm) = 0.017) sample of CBPHAT and a concentrated (OD (383 nm) = 0.48) one without and with 200 μ l 0.1 M of NaOH in 3 ml of DMF solution. For emission, the excitation wavelength was 370 nm.

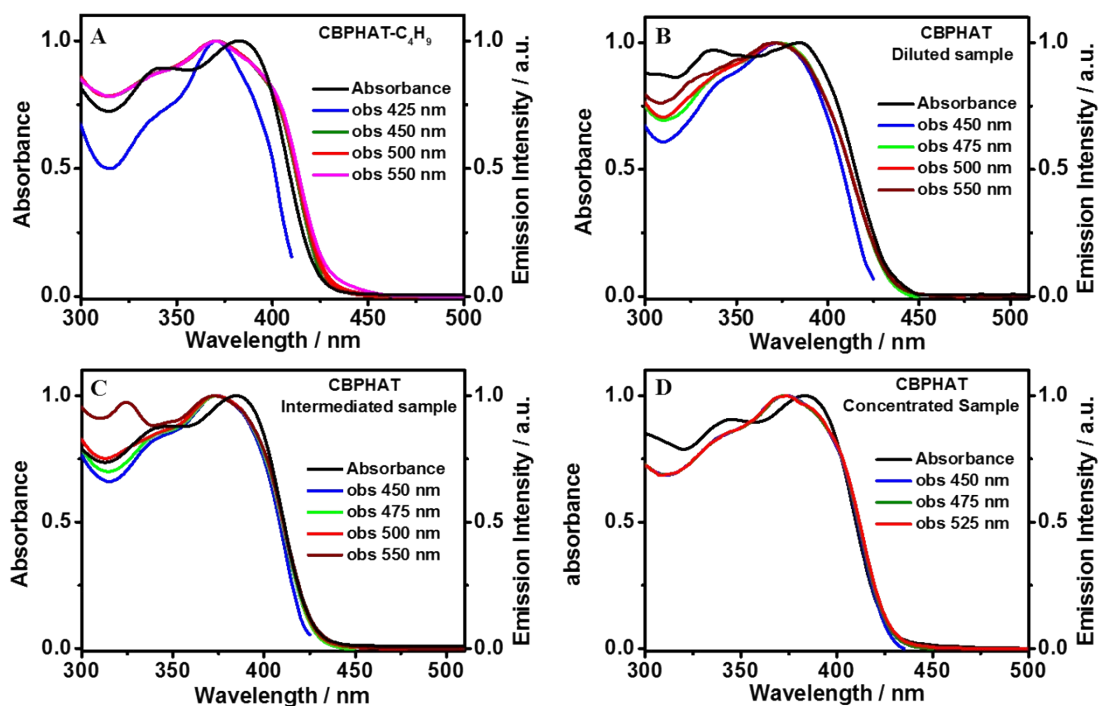


Figure S4. Normalized UV-visible absorption and excitation spectra of A) CBPHAT- C_4H_9 , B-D) CBPHAT at different concentrations in DMF solutions. The gated observation wavelengths are in the insets. The OD (383 nm) = 0.017, 0.31 and 0.48 for diluted, intermediate and concentrated samples, respectively).

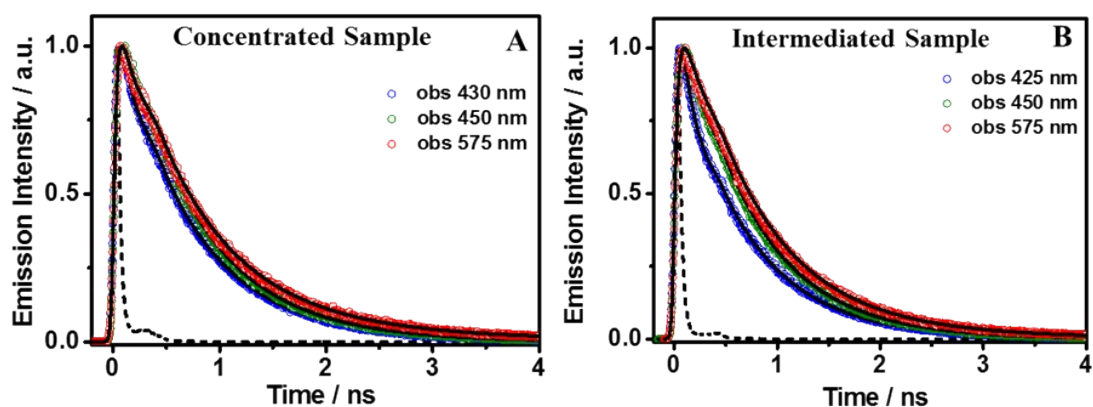


Figure S5. Normalized magic-angle emission decays of different samples having an OD (383 nm) of 0.48 and 0.31 of CBPHAT in DMF solutions upon excitation at 371 nm, and recording at indicated wavelengths. The solid lines are from the best global fits using a multiexponential function.

Sample	λ_{obs} (nm)	τ_1 (ps) ± 15 ps	A_1	c_1	τ_2 (ps) ± 20 ps	A_2	c_2	τ_3 (ns) ± 0.1 ns	A_3	c_3
CBPHAT diluted	425		59	24		40	72		1	4
	450		45	14		48	64		7	22
	475		30	7		54	56		16	37
	500	230	17	4	1.03	57	48	2.27	26	48
	525		9	1		54	39		37	60
	550		-	-		52	33		48	67
	575		-	-		42	24		58	76
CBPHAT	425		39	10		61	90		-	-
	450		10	1		80	82		10	17
	475		5	1		83	81		13	18
	500	90	-	-	664	82	74	1.01	18	26
	525		-	-		70	60		30	40
	550		-	-		62	51		38	49
	575		-	-		58	42		42	58

Table S2. Values of time constants (τ_i), normalized (to 100) pre-exponential factors (a_i) and contributions ($c_i = \tau_i \times a_i$) in the signal obtained from a global multiexponential fit of the emission decays of an intermediate concentration (OD (383 nm) = 0.31) of CBPHAT in a DMF solution. The excitation was at 371 nm, and observation as indicated.

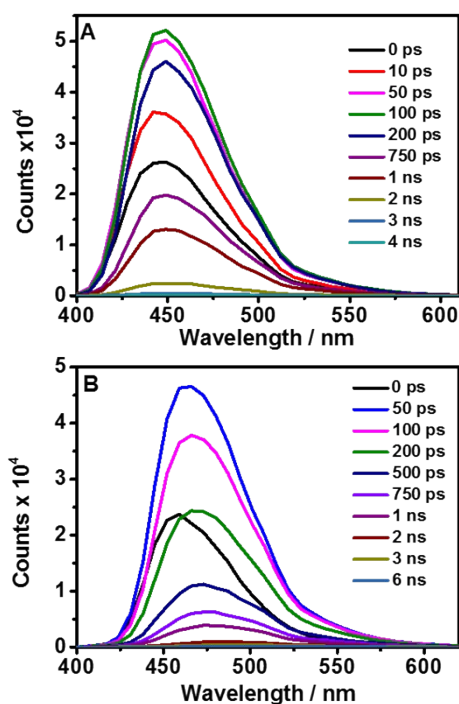


Figure S6. Time-resolved emission-spectra (TRES) of A) CBPHAT-C₄H₉ and B) CBPHAT (diluted, (OD (383 nm) = 0.017)) in DMF solutions. The excitation wavelength was 371 nm.

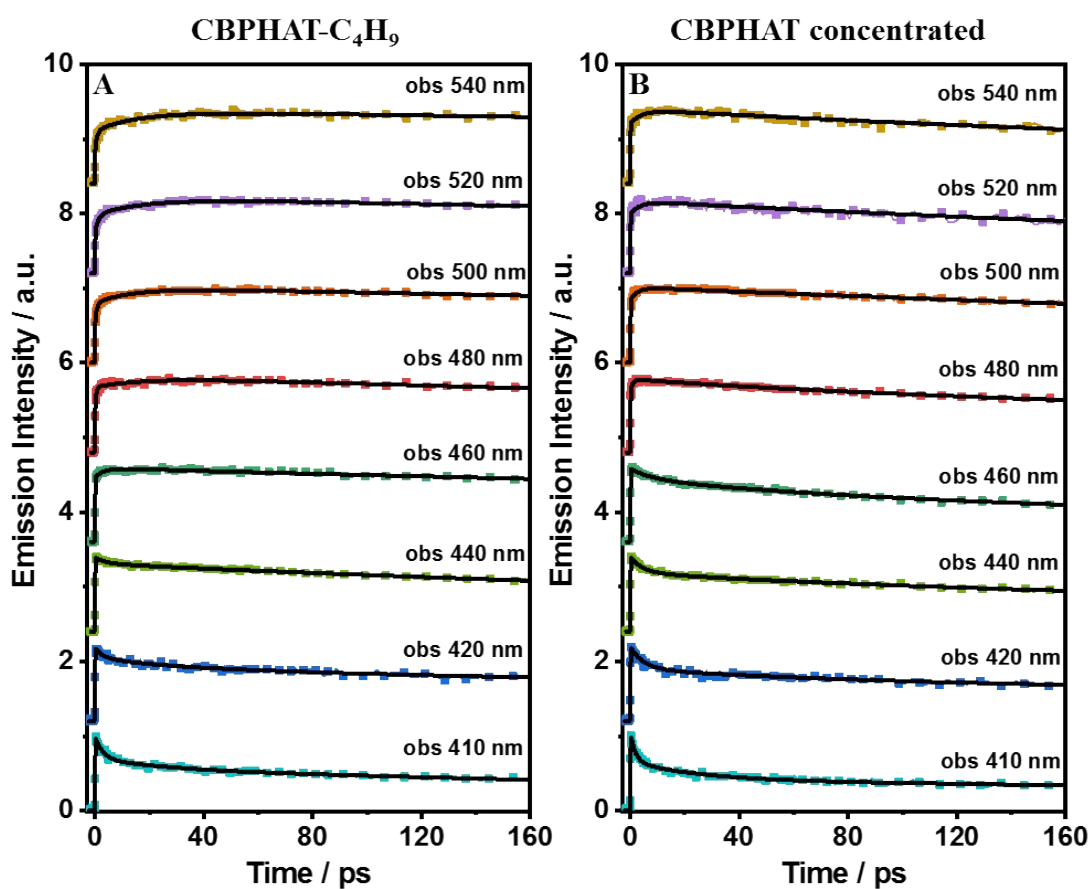


Figure S7. Fs-emission transients at longer time window of A) CBPHAT-C₄H₉ and B) concentrated sample (OD (383 nm) = 0.48) of CBPHAT in DMF solutions, upon excitation at 370 nm. The observation wavelengths are indicated in the inset. The solid lines are from the best fit using a multiexponential function.

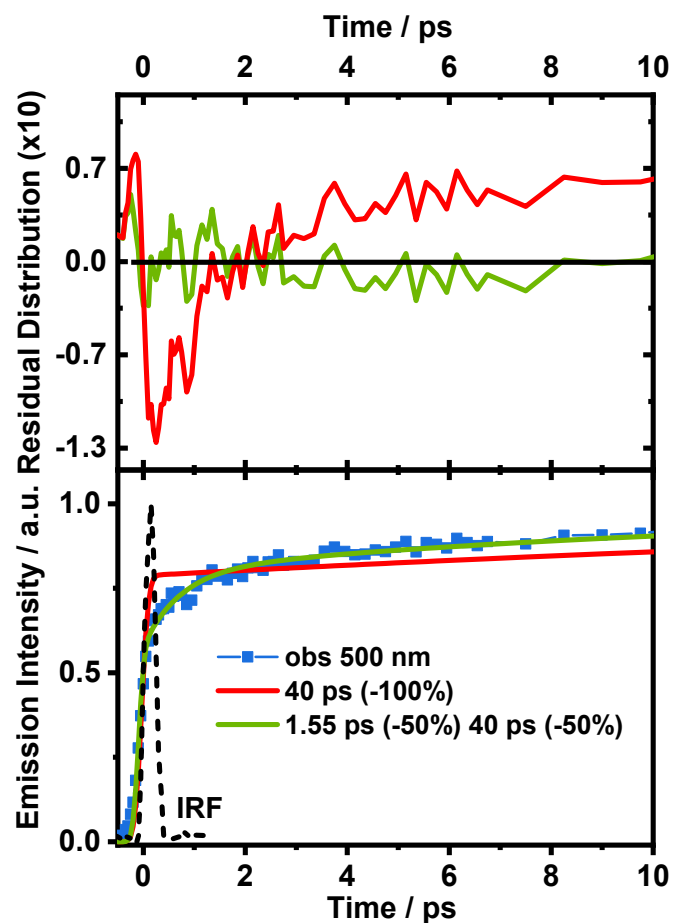


Figure S8. Fs-emission transient of CBPHAT-C₄H₉ observing at 500 nm in DMF solutions, upon excitation at 370 nm. The solid lines are from two fits using a multiexponential function with one (red) or two (green) rising components. The upper panel shows the residual distributions of both fits. The dashed signal is the IRF of the setup.

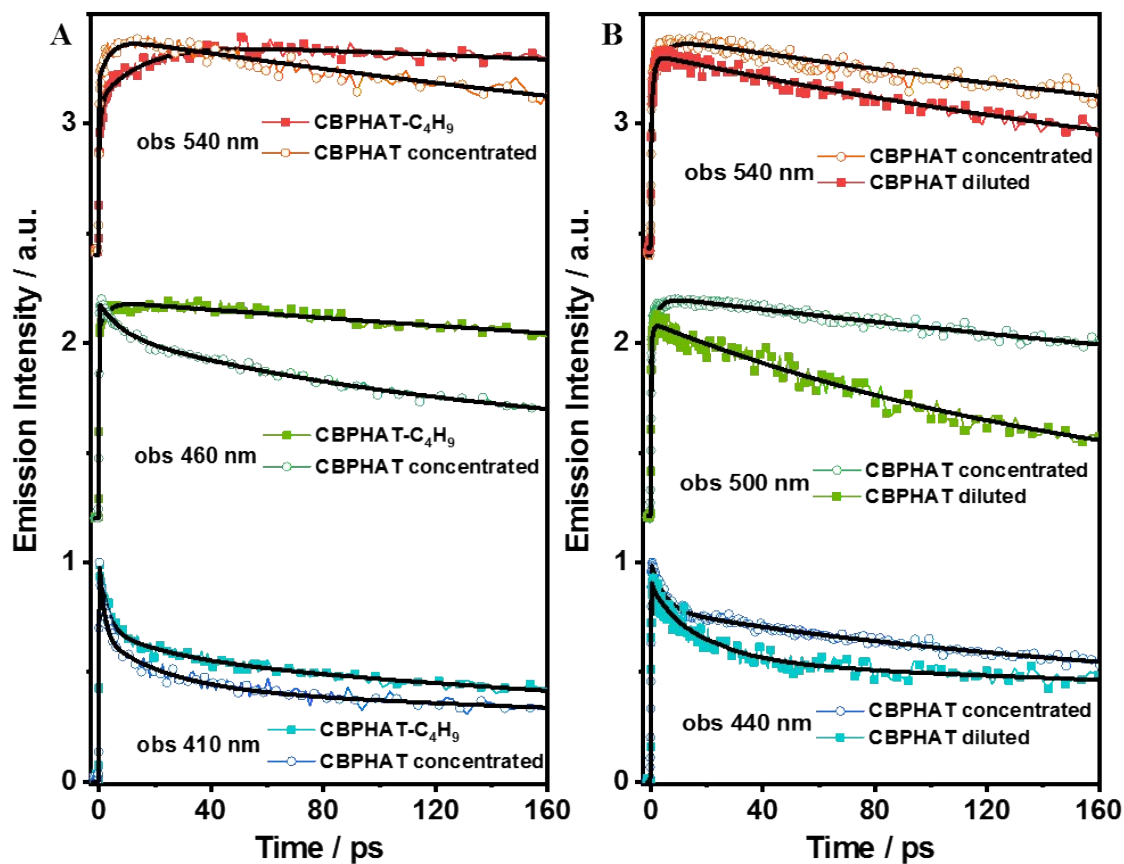


Figure S9. Comparison between fs-emission transients of A) CBPHAT-C₄H₉ and a concentrated (OD (383 nm) = 0.48) sample of CBPHAT in DMF solutions, and B) a concentrated (OD (383 nm) = 0.48) and diluted (OD (383 nm) = 0.017) sample of CBPHAT in DMF solutions, upon excitation at 370 nm. The observation wavelengths are indicated in the inset. The solid lines are from the best fit using a multiexponential function.

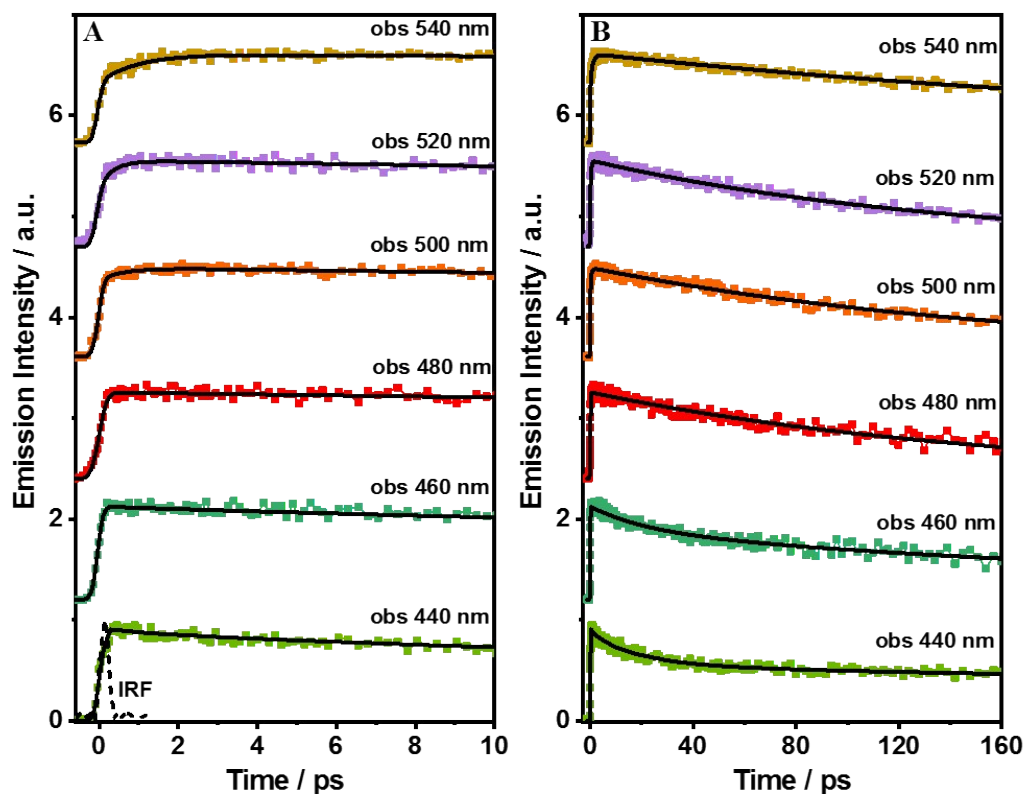


Figure S10. Fs-emission transients at A) short and B) long time window of a diluted sample (OD (383 nm) = 0.017) of CBPHAT in DMF solutions, upon excitation at 370 nm. The observation wavelengths are indicated in the inset. The solid lines are from the best fit using a multiexponential function. The dashed signal is the IRF of the setup.

Sample	λ_{obs} (nm)	τ_1 (ps) ± 0.5 ps	A_1	τ_2 (ps) ± 10 ps	A_2	τ_3 (ps)	A_3
CBPHAT diluted	440	-	-	32	67		33
	460	-	-	32	60		40
	480	-	-	35	31	230*	69
	500	0.9	-100	36	22		78
	520	1.0	-100	36	19		81
	540	1.4	-100	-	-		100

Table S3. Values of time constants (τ_i) and normalized (to 100) pre-exponential factors (ai) of the function used in fitting the fs-emission transients of a diluted sample (OD (383 nm) = 0.017) of CBPHAT in a DMF solution, upon excitation at 370 nm and observation as indicated. The negative sign of a_i indicates a rising component in the emission signal.

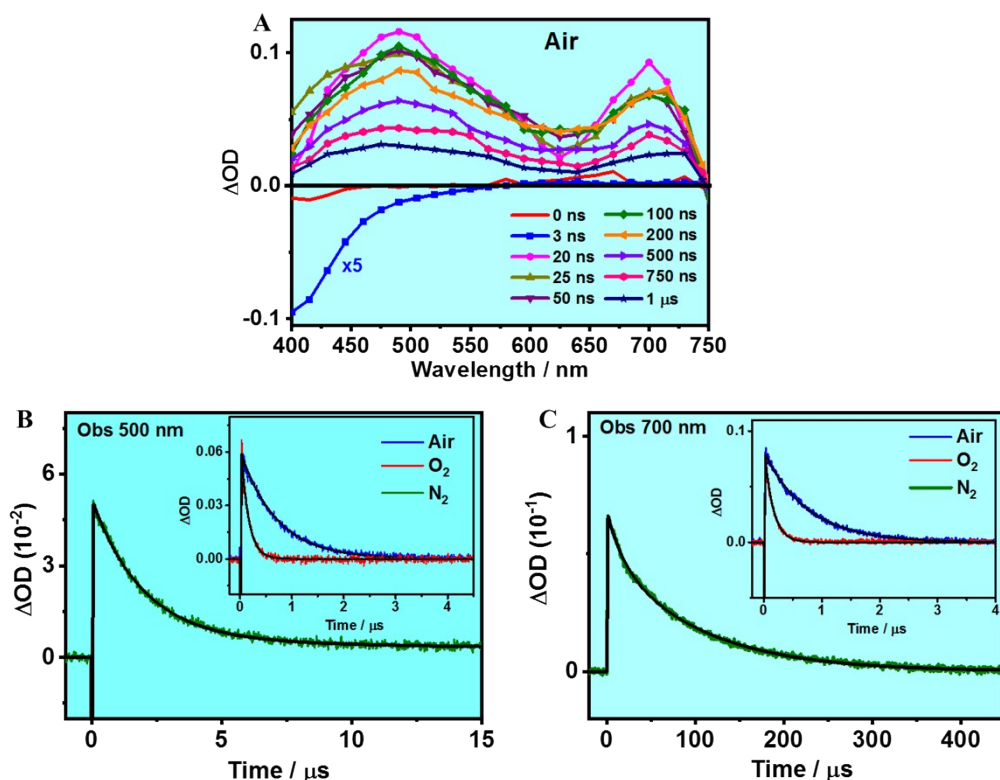


Figure S11. A) Time-resolved transient absorption spectra (in terms of ΔOD) of CBPHAT- C_4H_9 in DMF at different delay times upon excitation at 355 nm. B) and C) Transient absorption decays at 500 and 700 nm, under different atmospheric conditions: air (blue), oxygen (red) and nitrogen (green).

λ_{obs} (nm)	Conditions	τ_1 (μs) $\pm 0.1 \mu s$	A_1	τ_2 (μs) $\pm 10 \mu s$	c_2
500	Air	0.70	100		
	O ₂	0.14	100	-	-
	N ₂	1.95	100		
700	Air	0.75	100	-	-
	O ₂	0.15	100	-	-
	N ₂	17.6	74	101	26

Table S4. Values of time constants (τ_i) and normalized (to 100) pre-exponential factors (ai) obtained from the fit of the transient absorption decays of CBPHAT- C_4H_9 in DMF solutions, upon excitation at 355 nm and observation as indicated.

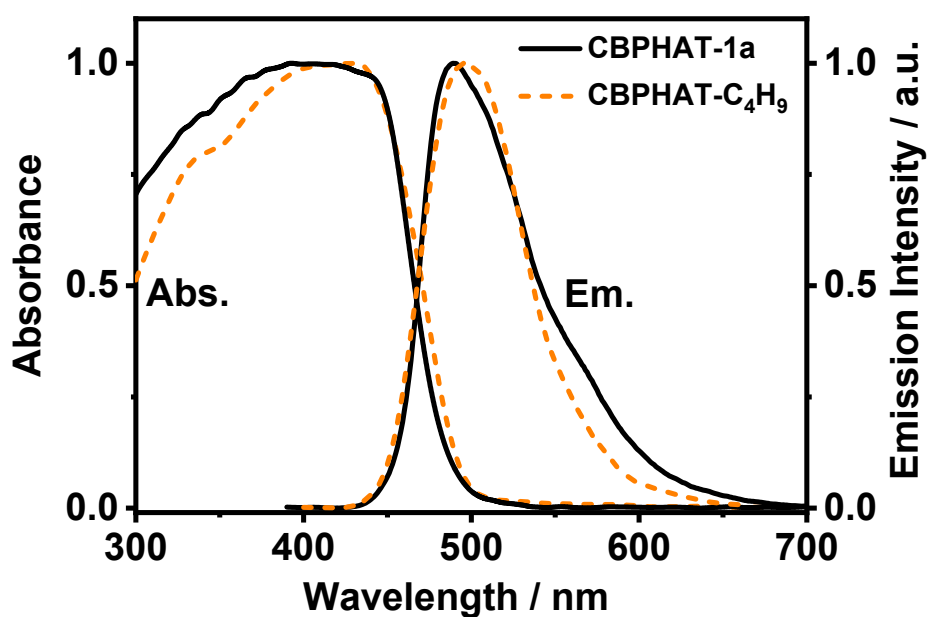


Figure S12. Normalized A) UV-visible absorption and emission spectra of CBPHAT- C_4H_9 and CBPHAT-1a in solid state. The excitation wavelength for both emission spectra was 370 nm.

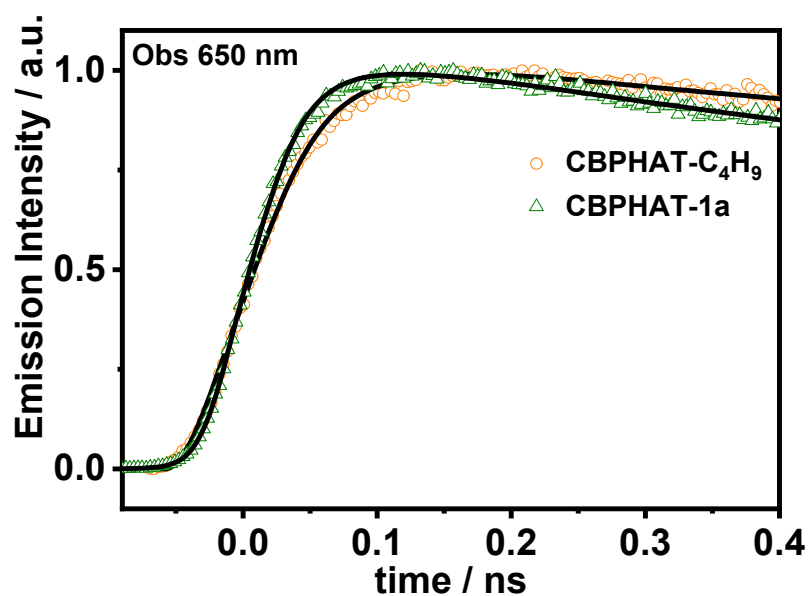


Figure S13. Normalized magic-angle emission decays of CBPHAT- C_4H_9 (orange circles) and CBPHAT-1a (green triangles) in DMF solutions upon excitation at 371 nm, and recording at 650 nm. The solid lines are from the best global fit using a multiexponential function. Note the difference in the rising component.

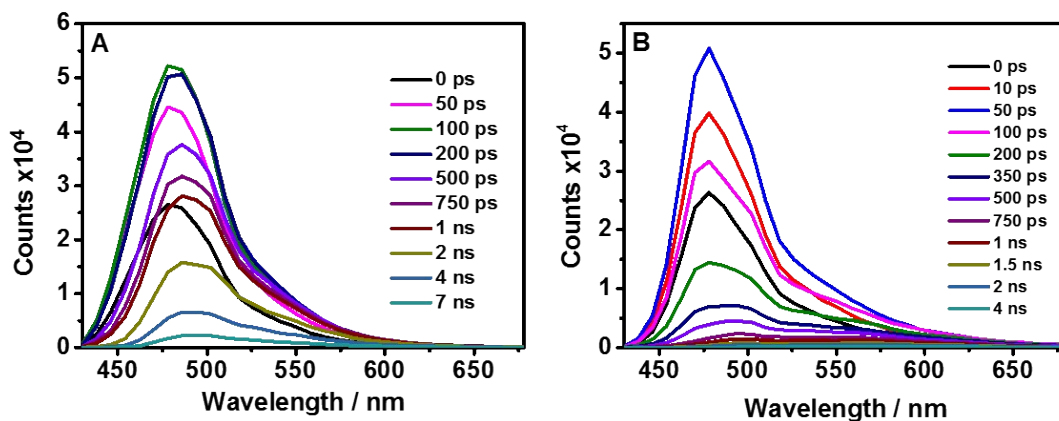


Figure S14. Time-resolved emission-spectra (TRES) of A) CBPHAT-C₄H₉ and B) CBPHAT-1a in solid state, upon excitation at 371 nm and gating at the indicated delay times.

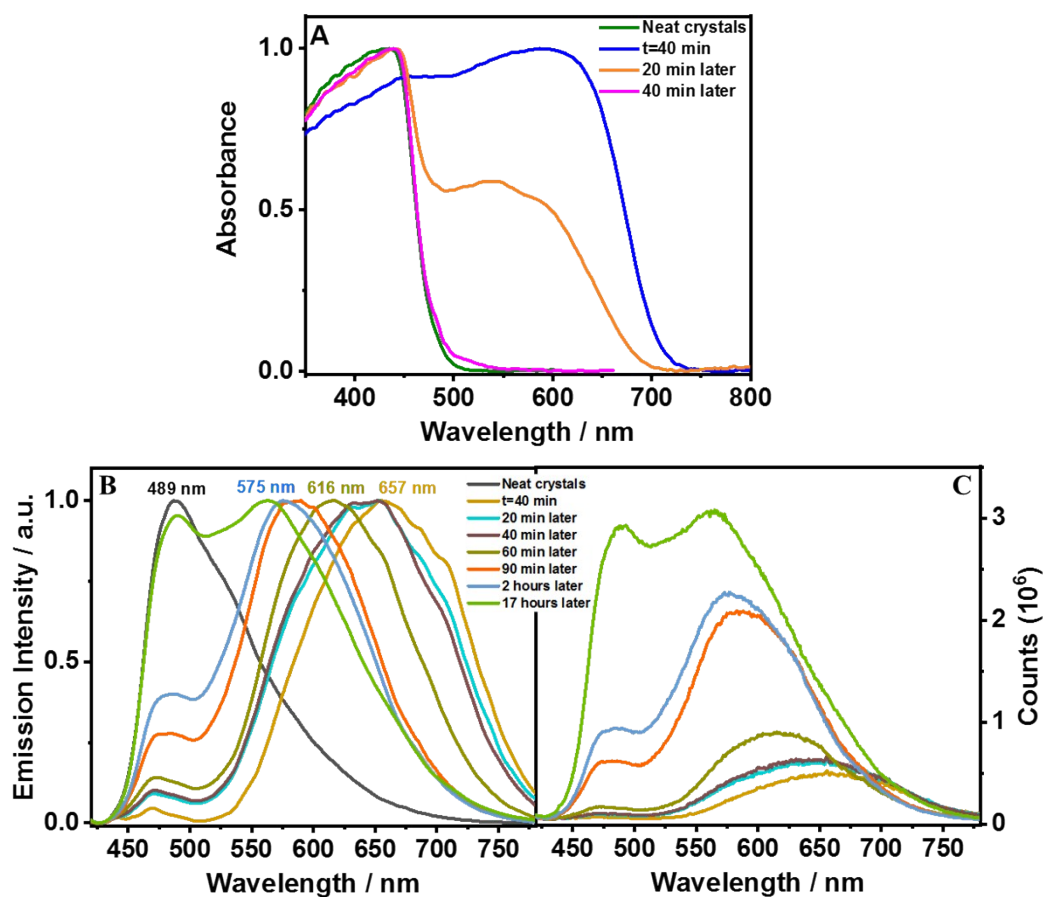


Figure S16. Normalized A) absorption and B) emission, and C) real emission spectra of CBPHAT-1a in solid state after 40 minutes in HCl atmosphere. The excitation wavelength for all emission spectra was 400 nm.

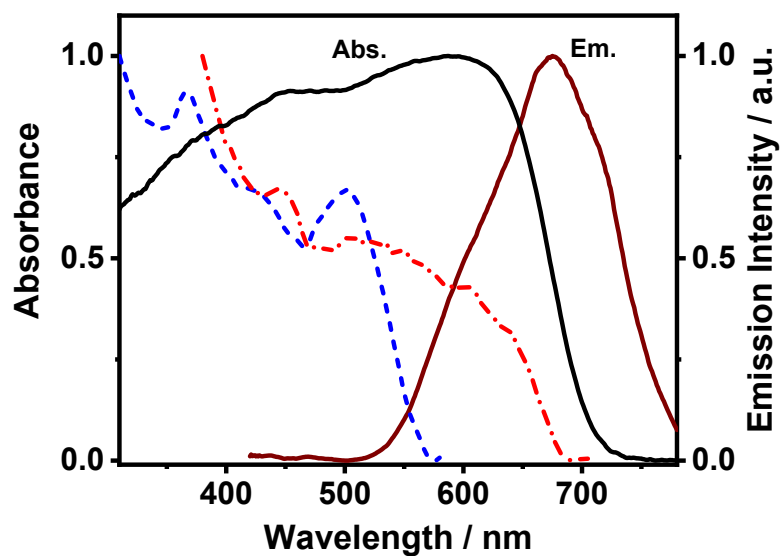


Figure S16. UV-visible absorption, emission (solid lines) and excitation spectra of CBPHAT-1a in solid state expose 30 minutes in HCl atmosphere and observing at 600 nm (dashed line) and 750 nm (dashed dotted line).

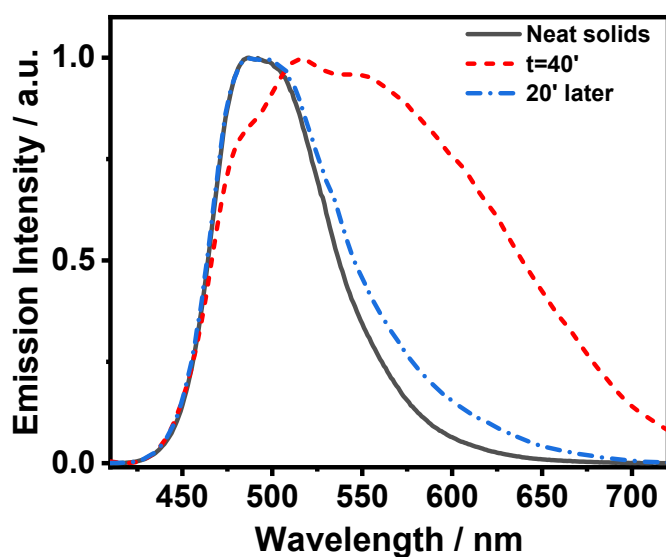


Figure S17. Normalized emission spectra of CBPHAT-C₄H₉ in solid state before and after 40 minutes in HCl atmosphere. The excitation wavelength was 400 nm.

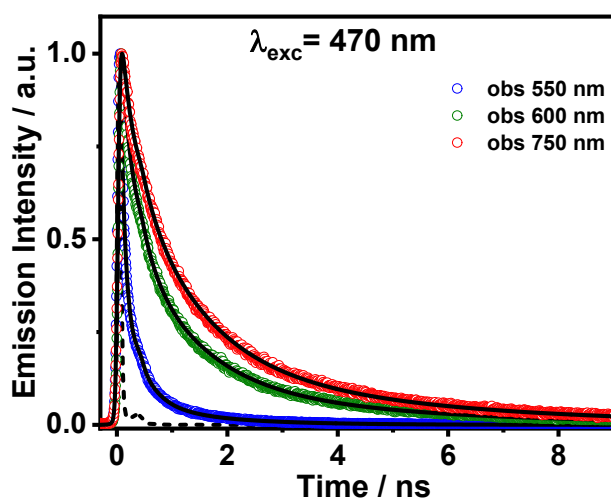


Figure S18. Magic-angle emission decays of CBPHAT-1a in solid state after 30 minutes in HCl atmosphere, upon excitation at 470 nm, and recording at the indicated wavelengths. The solid lines are from the best global fit using a multiexponential function. The dashed line is the IRF of the setup.

Sample	λ_{obs} (nm)	τ_1 (ps) ± 30 ps	A_1	c_1	τ_2 (ps) ± 50 ps	A_2	c_2	τ_3 (ns) ± 0.2 ns	A_3	c_3	τ_4 (ns) ± 0.3 ns	A_4	c_4
t= 5 min Exc=390 nm	450		82	48		17	43		1	9		-	-
	500		75	30		20	37		5	33		-	-
	550		70	28		20	37		10	35		-	-
	600	70	-	-	220	54	13	1.14	37	46	2.51	9	41
	650		-	-		46	10		42	45		12	45
	700		-	-		41	8		45	43		14	49
	750		-	-		40	7		45	43		15	50
t= 40 min Exc=390nm	550					77	29		20	44		3	27
	600					62	15		29	39		9	46
	650	-	-	-	100	58	13	630	32	40	2.31	10	47
	700					44	7		36	30		20	63
t= 40 min Exc=470nm	550					77	33		20	43		3	24
	600					61	16		32	45		7	39
	650	-	-	-	120	60	16	700	32	45	2.85	8	39
	700					45	8		36	32		19	60
	750					32	4		36	24		32	72

Table S5. Values of time constants (τ_i), normalized (to 100) pre-exponential factors (a_i) and contributions ($c_i = \tau_i \times a_i$) in the signal obtained from a global multiexponential fit of the emission decays of CBPHAT-1a after different times in HCl atmosphere.